

A HIGH-FLOW KNUDSEN PUMP USING A POLYMER MEMBRANE: PERFORMANCE AT AND BELOW ATMOSPHERIC PRESSURES

Naveen Kumar Gupta¹ and Yogesh B. Gianchandani

Department of Mechanical Engineering, University of Michigan, Ann Arbor, Michigan, USA

ABSTRACT

This paper describes a miniature gas (Knudsen) pump that utilizes thermomolecular flow through a nanoporous membrane. A temperature gradient along the length of a pore that supports free molecular gas flow at atmospheric pressure pumps gas molecules from the cold end to the hot end. In contrast with past work, the membrane material is mixed cellulose which provides superior uniformity in pore diameter and porosity. The final packaged volume of the Knudsen pump is 14x14x4.4 mm³. For an input power of 1.4 W, a single stage Knudsen pump based on these nanoporous polymer membrane has a temperature bias of 30 K across the thickness of the membrane, which provides 0.4 sccm flow against a 330 Pa pressure head. The load characteristics of the pump suggest that the pump can provide as much as 0.93 sccm gas flow in the absence of a load. Knudsen pump operation at sub-atmospheric pressures is also reported.

KEYWORDS

Knudsen pump, thermal transpiration, nanoporous polymer, gas flow, liquid flow.

INTRODUCTION

In the past five decades gas sensing and analysis systems have evolved from room-sized machines to table top devices, and continue to progress toward handheld microsystems. Miniaturization of (gas) pumps associated with these systems has emerged as an important challenge (Fig. 1) [1-3]. Many of the available options achieve miniaturization by compromising performance, reliability, or cost. Knudsen pumps, which are based on the phenomenon of thermal transpiration, can be potentially useful in addressing some of the challenges faced by existing micropumps [4]. Knudsen pumps have no moving parts; hence, they are potentially reliable and structurally simple.

The phenomenon of thermal transpiration was first studied by Reynolds and Maxwell, independently, in the year 1879 [5, 6]. In 1910, Knudsen demonstrated the possibility of using thermal transpiration for the purpose of gas pumping [7]. However, due to the unavailability of sufficiently small narrow channels, Knudsen pump operation at atmospheric pressure was

not demonstrated until quite recently [8, 9]. In our previous efforts, nanoporous ceramics have shown promise as thermal transpiration materials at atmospheric pressure. However, single stage Knudsen pumps based upon these could generate only a limited gas flow rate of 0.004 sccm/cm² [10].

Here we report the use of a nanoporous polymer membrane for thermal transpiration, which results in a 150x improvement in the gas flow with respect to our previous best case flow rates [10]. The phenomenon of thermal transpiration, the pump design and fabrication, and experimental results, are discussed in the following sections.

THERMAL TRANSPIRATION

The phenomenon of thermal transpiration refers to the ability of a narrow channel to sustain an equilibrium pressure gradient when subjected to a longitudinal temperature gradient [4, 11]. A narrow channel is defined as one in which the gas flow is in the free molecular or transitional regimes, that is, 0.1 < Kn < 10, and Kn > 10 respectively, where Kn, Knudsen number, is the ratio of the mean free path (λ) of gas molecules

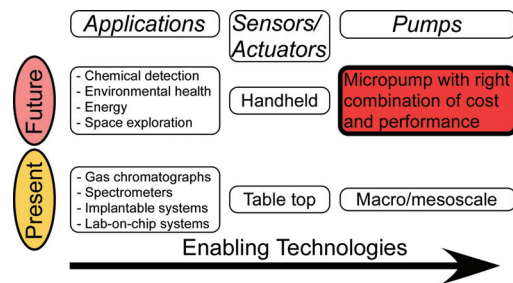


Fig. 1: Miniaturization of various handheld gas sensing and analysis systems depends largely on the availability of gas micropumps with necessary combination of performance and cost.

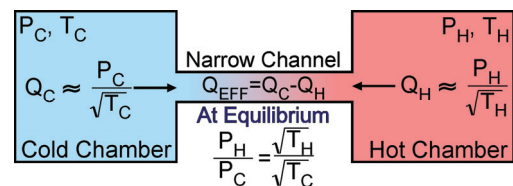


Fig. 2: Thermal transpiration between two chambers connected by a channel that permits flow only in the free molecular or transitional regimes. At equilibrium, the ratio of pressures in the two chambers is equal to the square root of the ratio of temperatures in the respective chambers.

¹ Contact: gnavveen@umich.edu, 1301 Beal, Ann Arbor, MI-48109

to the hydraulic diameter (d) of the channel such that $Kn = \lambda/d$ [12].

The concept of thermal transpiration can be simply explained by Figure 2. Suppose there are two chambers at unequal temperatures (T_H , T_C) that are connected by a narrow channel, the rate of gas flow from one chamber to another is directly proportional to the pressure in that chamber and inversely proportional to the square root of temperature of that chamber [4]. Hence, if the initial pressures in the two chambers are equal, there is an effective movement of gas molecules from the cold chamber to the hot chamber. At equilibrium, the relationship between the pressure in the hot chamber (P_H) and the cold chamber (P_C) is given by:

$$\frac{P_H}{P_C} = \sqrt{\frac{T_H}{T_C}} \quad (1)$$

Sharipov's model [13] is one of the most representative models for thermal transpiration driven gas flow through nanochannels [14]. It is applicable to practically all flow regimes. Sharipov's model suggests that for a nanochannel with hydraulic radius a and length l , the average gas flow rate through the nanochannel is:

$$\dot{M}_{avg} = \left[Q_T \frac{T_H - T_C}{T_{avg}} - Q_P \frac{P_H - P_C}{P_{avg}} \right] \frac{\pi a^3 P_{avg}}{l} \left[\frac{m}{2k_B T_{avg}} \right]^{1/2} \quad (2)$$

where T_{avg} and P_{avg} are the average temperature and pressure in the nanochannel; m is the mass of a gas molecule; k_B is the Boltzmann constant; Q_T and Q_P are the temperature and pressure gas flow coefficients, which depend on a rarefaction parameter:

$$\delta_{avg} = \left[\frac{\pi^3}{2} \right]^{1/2} \frac{aD^2 P_{avg}}{k_B T_{avg}} \quad (3)$$

where D is the collision diameter of the gas molecules flowing across the nanochannel. In general, if T and P are the temperature and pressure along the length of narrow channel and dT/dx and dP/dx are the respective gradients:

$$\frac{dP}{dx} = \frac{Q_T}{Q_P} \frac{P}{T} \frac{dT}{dx} \quad (4)$$

DEVICE STRUCTURE

A nanoporous polymer membrane comprised of mixed cellulose is used for thermal transpiration. The membrane, 105 μm thick and 11.5 mm in diameter, has an average nanopore diameter of 25 nm and porosity 70%. The membrane is sandwiched between a passively cooled brass base and a heated brass top (Fig. 3a). An insulating ring and cap provide lateral and top-side sealing, respectively. A thin resistive element (26.67 Ω), laminated between insulating layers of Kapton, is used to maintain the top brass at

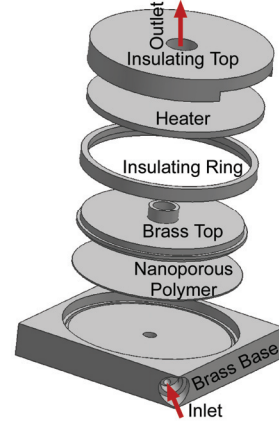


Fig. 3a: Exploded view of the polymer based Knudsen pump.

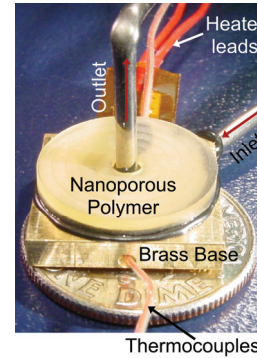


Fig. 3b: Packaged polymer based single stage Knudsen pump.

an elevated temperature. Thermocouples are embedded in the device to record the temperature drop across the membrane. Stainless steel capillaries are used at the inlet and at the outlet ports. The packaged volume of the final device is 14x14x4.4 mm³ (Fig. 3b).

EXPERIMENTAL RESULTS

Test Set-Up

The fabricated micropumps are tested in two modes. 1) *Flow mode*: A clear Tygon tube (0.79 mm ϕ), with water plugs, is connected at the inlet, while the outlet is open to the ambient. This mode is used to quantify the gas flow rate as a function of pressure head for a given input power. The pressure head is controlled by the size of the droplet in the Tygon tube. 2) *Pressure mode*: The device is located on a heat sink placed within a pressure-controlled chamber (PCC) that has an externally controlled pressure, P_{vc} . The inlet of the device is sealed, while the outlet is open to the PCC. The differential pressure between the sealed inlet and the PCC is monitored for different operating conditions.

Steady State Results

Figure 4 illustrates that the experimentally measured

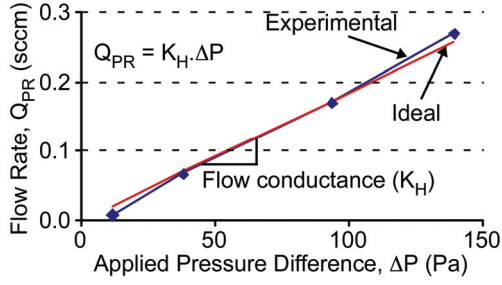


Fig. 4: The hydraulic conductance of the nanoporous membrane is measured using an externally applied pressure. The membrane is 105 μm thick, 11.5 mm in diameter and 70% porous. The nanopores are 25 nm in diameter.

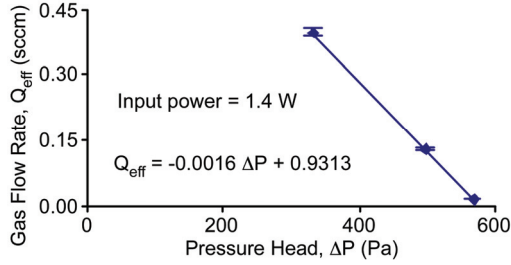


Fig. 5: Flow Mode Tests: Experimentally measured inlet flow rate for the Knudsen pump at 1.4 W input power, with varying pressure loads.

pressure driven gas flow across the membrane (Q_{PR}) increases linearly with (externally) applied differential pressure across these membranes (ΔP). The plot suggests that the membrane has a gas flow conductance (K_H) of $\approx 1.97 \times 10^{-3}$ sccm/Pa.

$$K_H = \frac{Q_{PR}}{\Delta P} \quad (5)$$

Figure 4 also shows that the ideal value for K_H , calculated using the nominal values for the membrane parameters (Eqn. 2), fits closely with the experimentally measured K_H – with less than 5% deviation.

Flow Mode Testing: Two types of flow fields co-exist in a Knudsen pump: one is the temperature gradient driven thermal transpiration flow (Q_{TT}) from the cold side of the membrane to the hot side, while the other is the pressure gradient-driven gas flow across the membrane (Q_{PR}) from the hot side of the membrane to the cold side. The net flow (Q_{eff}) is the algebraic sum of these two gas flow rates, that is:

$$Q_{eff} = Q_{TT} - Q_{PR} \quad (6)$$

Figure 5 shows the experimentally measured gas flow generated by the device (Q_{eff}) with pressure load (ΔP) at the inlet. The input power was held constant at 1.4 W for this experiment. With reduction in pressure load, the gas flow rate increases linearly to an extrapolated no load flow of ≈ 0.93 sccm.

Pressure Mode Testing: As mentioned earlier, inlet of a Knudsen pump is sealed while testing it in pressure

mode. This implies that the steady state gas flow rate across its membrane is zero: $Q_{eff} = 0$. Hence, $Q_{TT} = Q_{PR} = K_H \cdot \Delta P$. This value of Q_{TT} can, therefore, be extracted from the Pressure Mode Tests. As shown in Fig. 6, Q_{TT} may exceed 1.2 sccm for a temperature bias as low as $\approx 30\text{K}$ across the membrane, with average operating temperatures smaller than 333K. The pumping rate Q_{TT} decreases linearly with temperature bias. These flow rates are higher than those measured for similar conditions in the *Flow Mode Tests* because the flow mode results must accommodate the flow resistance at the membrane and brass top/base interfaces.

Figure 7 shows that the differential vacuum pressure generated by the device (at the sealed inlet) increases linearly with the temperature difference across the nanoporous membrane. At atmospheric pressure ($P_{vc} = 98.5$ kPa), a temperature bias of 30K across the nanoporous membrane results in pressure drop >620 Pa. The differential pressure drop generated by the pump reduces significantly as P_{vc} is lowered from the atmospheric pressure (98.5 kPa) to 6.7 kPa.

Transient Results

Pressure Mode: Pressure mode operation of the

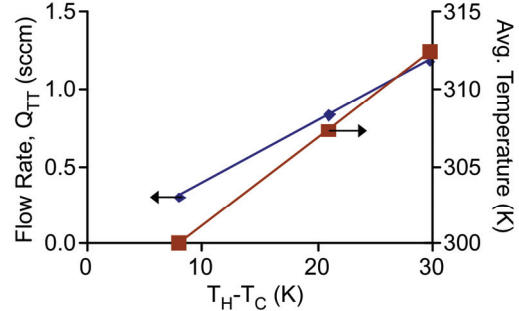


Fig. 6: Pressure Mode Testing: Thermal transpiration Q_{TT} driven gas flow is same as the pressure driven gas flow Q_{PR} across the membrane. The product of the hydraulic conductance K_H of the membrane and the pressure head ΔP generated by the pump gives an estimate of Q_{PR} .

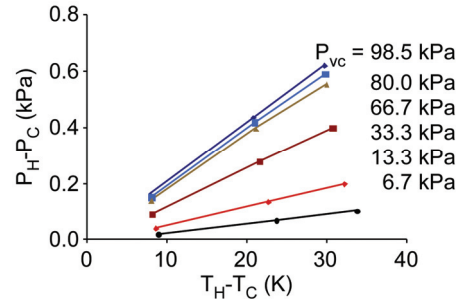


Fig. 7: Pressure Mode Testing: Measured pressure head generated by the pump for different ambient operating pressures of the device.

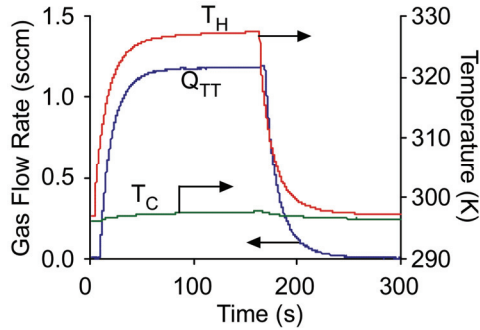


Fig. 8: Pressure Mode Testing: Effective gas flow into the cold chamber Q_{eff} , derived from the time derivative of pressure at the sealed inlet, is compensated for the pressure driven back flow Q_{PR} due to the vacuum pressure $P_{\text{H}}-P_{\text{C}}$ to estimate the temporal evolution of thermal transpiration driven gas flow Q_{TT} generated by the pump.

Knudsen pump yields the temporal evolution of the differential vacuum pressure $\Delta P(t)$ at the sealed inlet. The volume of the sealed inlet, including the cold chamber and the attached tubing, is 0.472 cm^3 . The time derivative of $\Delta P(t)$ is proportional to the gas pumped out of the cold chamber $Q_{\text{eff}}(t)$. Equation 5 is used to estimate $Q_{\text{PR}}(t)$ using K_{H} and $\Delta P(t)$. Sum of $Q_{\text{PR}}(t)$ and $Q_{\text{eff}}(t)$ provides the temporal evolution of the thermal transpiration flow $Q_{\text{TT}}(t)$ (Eqn. 6, Fig. 8). Figure 8 also shows the temporal evolution of the hot (T_{H}) and cold (T_{C}) end temperatures of the device.

CONCLUSION

This work shows that nanoporous polymer membranes are promising for generating flow rates on the order of 1 sccm at operating temperature biases of 30K. Unlike bulk nanoporous ceramics, these membranes offer high thermal isolation, and hence permit reasonable thermal efficiency. A Knudsen pump based on a mixed cellulose polymer membrane, with pore size 25 nm and porosity 70%, resulted in a gas flow rate of 0.4 sccm. Load-flow characteristics suggest a no load gas flow rate of 0.93 sccm, which is potentially useful for several microfluidic systems [15]. The temporal evolution of pressure in the cold chamber suggests that the transient response of the pump is limited by the thermal response of the device rather than the thermal transpiration driven gas flow through the membranes.

ACKNOWLEDGEMENT

NG acknowledges partial support by a fellowship from the Mechanical Engineering department. The study is supported in part by Defense Advanced Research Projects Agency High-Vacuum Program (DARPA Hi-Vac).

REFERENCES

- [1] D.J. Laser, J.G. Santiago, "A Review of Micropumps," *J. Micromechanics and Microengineering*, 14(6), 2004, pp. R35-R64.
- [2] H. Kim, A.A. Astle, K.Najafi, L.P. Bernal, P.D. Washabaugh, "A Fully Integrated High-Efficiency Peristaltic 18-Stage Gas Micropump with Active Microvalves," *IEEE Intl. Conf. on Micro Electro Mechanical Systems (MEMS)*, 2007, pp. 127-30.
- [3] C.G.J. Schabmuller, M. Koch, M.E. Mokhtari, A.G.R. Evans, A. Brunnschweiler, H. Sehr, "Self-Aligning Gas/Liquid Micropump," *J. Micromechanics and Microengineering*, 12(4), 2002, pp. 420-424.
- [4] L. Loeb, *The Kinetic Theory of Gases*, McGraw Hill, 1934, pp. 355-359.
- [5] O. Reynolds, "On Certain Dimensional Properties of Matter in the Gaseous State," *Phil. Trans. of Royal Society London*, 170, 1879, pp. 727-845.
- [6] J.C. Maxwell, "On Stresses in Rarefied Gases Arising from Inequalities of Temperature," *Phil. Trans. Royal Society London*, 170, 1879, pp. 231-256.
- [7] M. Knudsen, "Eine Revision der Gleichgewichtsbedingung der Gase. Thermische Molekularstromung," *Annalen der Physik*, Leipzig, 336(1), 1909, pp. 205-229.
- [8] S.E. Vargo, E.P. Muntz, "Initial Results from the First MEMS Fabricated Thermal Transpiration-Driven Vacuum Pump," *AIP Conference Proceedings*, 585, 2001, pp. 502-509.
- [9] S. McNamara, Y.B. Gianchandani, "On-Chip Vacuum Generated by a Micromachined Knudsen Pump," *J. Microelectromechanical Systems*, 14(4), 2005, pp. 741-746.
- [10] N.K. Gupta, Y.B. Gianchandani, "Thermal Transpiration in Zeolites: A Mechanism for Motionless Gas Pumps," *Applied Physics Letters*, 93(19), 2008, p. 193511.
- [11] E. Kennard, *Kinetic Theory of Gases*, McGraw Hill, 1938, pp. 327-332.
- [12] G.E. Karniadakis, A. Beskok, N. Aluru, *Microflows and Nanoflows: Fundamentals and Simulation*, Springer, New York, 2005, Chap. 1.
- [13] F. Sharipov, "Rarefied Gas Flow Through a Long Tube at Arbitrary Pressure and Temperature Drop," *J. Vacuum Science and Technology A*, 15(4), 1997, pp. 2434-2436.
- [14] N.K. Gupta, N.D. Masters, W. Ye, Y.B. Gianchandani, "Gas Flow in Nano-Channels: Thermal Transpiration Models with Application to a Si-Micromachined Knudsen Pump," *IEEE Intl. Conf. on Solid State Sensors, Actuators, and Microsystems (Transducers)*, 2007, pp. 2329-2332.
- [15] S. Sia, G. Whitesides, "Microfluidic Devices Fabricated in Poly(dimethylsiloxane) for biological studies," *Electrophoresis*, 24, 2003, pp. 3563-76.